

# Contrastively Smoothed Class Alignment for Unsupervised Domain Adaptation

Shuyang Dai<sup>1</sup> Yu Cheng<sup>2</sup> Yizhe Zhang<sup>2</sup> Zhe Gan<sup>2</sup> Jingjing Liu<sup>2</sup> Lawrence Carin<sup>1</sup>

<sup>1</sup>Duke University <sup>2</sup>Microsoft Dynamics 365 AI Research

{shuyang.dai, lcarin}@duke.edu

{yu.cheng, yizhe.zhang, zhe.gan, jingjl}@microsoft.com

## Abstract

Recent unsupervised approaches to domain adaptation primarily focus on minimizing the gap between the source and the target domains through refining the feature generator, in order to learn a better alignment between the two domains. This minimization can be achieved via a domain classifier to detect target-domain features that are divergent from source-domain features. However, by optimizing via such domain classification discrepancy, ambiguous target samples that are not smoothly distributed on the low-dimensional data manifold are often missed. To solve this issue, we propose a novel Contrastively Smoothed Class Alignment (CoSCA) model, that explicitly incorporates both intra- and inter-class domain discrepancy to better align ambiguous target samples with the source domain. CoSCA estimates the underlying label hypothesis of target samples, and simultaneously adapts their feature representations by optimizing a proposed contrastive loss. In addition, Maximum Mean Discrepancy (MMD) is utilized to directly match features between source and target samples for better global alignment. Experiments on several benchmark datasets demonstrate that CoSCA can outperform state-of-the-art approaches for unsupervised domain adaptation by producing more discriminative features.

## Introduction

Deep neural networks (DNNs) have significantly improved the state of the art on many supervised tasks (Donahue et al. 2014; Yosinski et al. 2014; Simonyan and Zisserman 2015; He et al. 2016). However, without sufficient training data, DNNs have weak generalization ability to new tasks or new environments (Torralba and Efros 2011). This is known as the dataset bias or domain-shift problem (Gretton et al. 2009). Unsupervised domain adaptation (UDA) (Pan et al. 2010; Ganin et al. 2016) aims to generalize a model learned from a source domain with rich annotated data to a new target domain without any labeled data. Recently, many approaches have been proposed to learn transferable representations, by simultaneously matching feature distributions across different domains (Haeusser et al. 2017; Tzeng et al. 2015).

Motivated by (Goodfellow et al. 2014), (Tzeng et al. 2017; Ganin and Lempitsky 2014) introduced a min-max game: a domain discriminator is learned by minimizing the error of

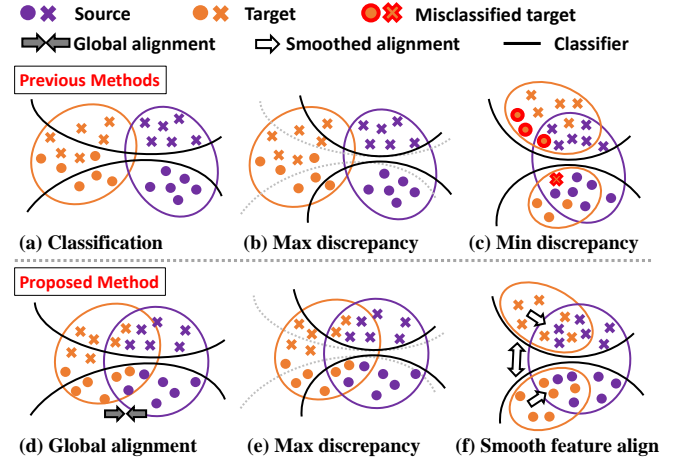


Figure 1: Comparison between previous classifier-discrepancy-based methods and our proposed CoSCA in the *feature* space. **Top:** The region of vacancy created by maximum discrepancy reduces the smoothness of alignment between ambiguous target samples and source samples, leading to sub-optimal solutions. This problem becomes more severe when global domain alignment is not considered. **Bottom:** Demonstration of global alignment and class-conditional adaptation by using the proposed CoSCA. After classifier discrepancy is maximized, the proposed contrastive loss moves ambiguous target samples near the decision boundary towards their neighbors and separates them from non-neighbors.

distinguishing data samples from the source and the target domains, while a feature generator learns transferable features that are indistinguishable by the domain discriminator. This enforces that the learned features be domain-invariant. Meanwhile, a feature classifier (only on source-domain features) ensures that the learned features are class-conditional. Despite promising results, these adversarial methods suffer from inherent algorithmic weaknesses (Shu et al. 2018). Specifically, the generator may generate ambiguous features near class boundaries (Saito et al. 2018): while the generator manages to fool the discriminator, some target-domain features may still be misclassified. In other words, the model merely aligns the global marginal distribution of the two domains and ignores the class-conditional decision boundaries.

To overcome this issue, recent UDA models further align

class-level distributions by taking the decision boundary into consideration. These methods either rely on iteratively refining the decision boundary with empirical data (Shu et al. 2018; Saito et al. 2017a), or utilizing multiple-view information (Kumar et al. 2018). Alternatively, the maximum classifier discrepancy (MCD) model (Saito et al. 2018) conducts a min-max game between a feature generator and two classifiers. Ambiguous target samples that are far from source-domain samples can be detected when the discrepancy between the two classifiers is maximized, as shown in Figure 1(b). Meanwhile, as the generator fools the classifiers, the generated target features may fall into the source feature regions. However, the target samples may not be smooth on the low-dimensional manifold (Chapelle et al. 2009; Luo et al. 2017), meaning that neighboring samples may not belong to the same class. As a result, some generated target features could be miscategorized as shown in Figure 1(c).

We propose the **Contrastively Smoothed Class Alignment (CoSCA)** model to improve the alignment of class-conditional feature distributions between source and target domains, by alternatively estimating the underlying label hypothesis of target samples to map them into tighter clusters, and adapting feature representations based on a proposed contrastive loss. Specifically, by aligning ambiguous target samples near the decision boundaries with their neighbors and distancing them from non-neighbors, CoSCA enhances the alignment of each class in a contrastive manner. Figure 1(f) demonstrates an enhanced and smoothed version of the class-conditional alignment. Moreover, as shown in Figure 1(d), Maximum Mean Discrepancy (MMD) is included to better merge the source and target domain feature representations. The overall framework is trained end-to-end in an adversarial manner.

Our main contributions are summarized as follows:

- We propose CoSCA, a novel approach that smooths class alignment for maximizing classifier discrepancy with a contrastive loss. CoSCA also provides better global domain alignment via the use of MMD loss.
- We validate the proposed approach on several domain adaptation benchmarks. Extensive experiments demonstrate that CoSCA achieves state-of-the-art results on several benchmarks.

## Related Work

**Unsupervised Domain Adaptation.** A practical solution for domain adaptation is to learn domain-invariant features whose distribution is similar across the source and target domains. For example, (Sener et al. 2016) designed discriminative features by using clustering techniques and pseudo-labels. DAN (Long et al. 2015) and JAN (Long et al. 2016) minimized the MMD loss between two domains. Adversarial domain adaptation was proposed to integrate adversarial learning and domain adaptation in a two-player game (Ganin and Lempitsky 2014; Tzeng et al. 2017; 2015). Following this idea, most existing adversarial-learning methods reduce feature differences by fooling a domain discriminator (Long et al. 2018; Ganin et al. 2016). However, the relationship between target samples and the class-conditional decision

boundaries when aligning features (Saito et al. 2018) was not considered.

**Class-conditional Alignment.** Recent work enforces class-level alignment while aligning global marginal distributions. Adversarial Dropout Regularization (ADR) (Saito et al. 2017a) and Maximum Classifier Discrepancy (MCD) (Saito et al. 2018) were proposed to train a neural network in an adversarial manner, avoiding generating non-discriminative features lying in the region near the decision boundary. (Pei et al. 2018; Long et al. 2016) considered class information when measuring domain discrepancy. Co-regularized Domain Adaptation (Co-DA) (Kumar et al. 2018) utilized multi-view information to match the marginal feature distributions corresponding to the class-conditional distributions. Compared with previous work that executed the alignment by optimizing on “hard” metrics (Saito et al. 2018; Kumar et al. 2018), we propose to smooth the alignment iteratively, with explicitly defined loss.

**Contrastive Learning.** The intuition for contrastive learning is to let the model understand the difference between one set (*e.g.*, data points) and another, instead of only characterizing a single set (Zou et al. 2013). This idea has been explored in previous works that model intra-class compactness and inter-class separability (*e.g.*, distinctiveness loss (Dai and Lin 2017), contrastive loss (Hadsell et al. 2006), triplet loss (Wang et al. 2014)) and tangent distance (Rifai et al. 2011). It has also been extended to consider several assumptions in semi-supervised and unsupervised learning (Luo et al. 2017; Li et al. 2017), such as the low-density region (or cluster) assumption (Luo et al. 2017; Rifai et al. 2011) that the decision boundary should lie in the low-density region, rather than crossing the high-density region. Recently, contrastive learning was applied in UDA (Kang et al. 2019), in which the intra/inter-class domain discrepancy were modeled. In comparison, our work is based on the MCD framework, utilizing the low-density assumption and focusing on separating the ambiguous target data points by optimizing the contrastive objective, allowing the decision boundary to sit in the low-density region, *i.e.*, region of vacancy, and smoothness assumption.

## Approach

The task of unsupervised domain adaptation seeks to generalize a learned model from a source domain to a target domain, the latter following a different (but related) data distribution from the former. Specifically, the source- and target-domain samples are denoted  $\mathcal{S} = \{(\mathbf{x}_1^s, y_1^s), \dots, (\mathbf{x}_i^s, y_i^s), \dots, (\mathbf{x}_{N_s}^s, y_{N_s}^s)\}$ , and  $\mathcal{T} = \{\mathbf{x}_1^t, \dots, \mathbf{x}_i^t, \dots, \mathbf{x}_{N_t}^t\}$ , respectively, where  $\mathbf{x}_i^s$  and  $\mathbf{x}_i^t$  are the input, and  $y_i^s \in \{1, 2, \dots, K\}$  represents the data labels of  $K$  classes in the source domain. The target domain shares the same label types as the source domain, but we possess no labeled examples from the target domain. We are interested in learning a deep network  $G$  that reduces domain shift in the data distribution across  $\mathcal{S}$  and  $\mathcal{T}$ , in order to make accurate predictions for  $y_i^t$ . We use the notation  $(\mathbf{X}^s, \mathbf{Y}^s)$  to describe the source-domain samples and labels, and  $\mathbf{X}^t$  for the unlabeled target-domain samples.

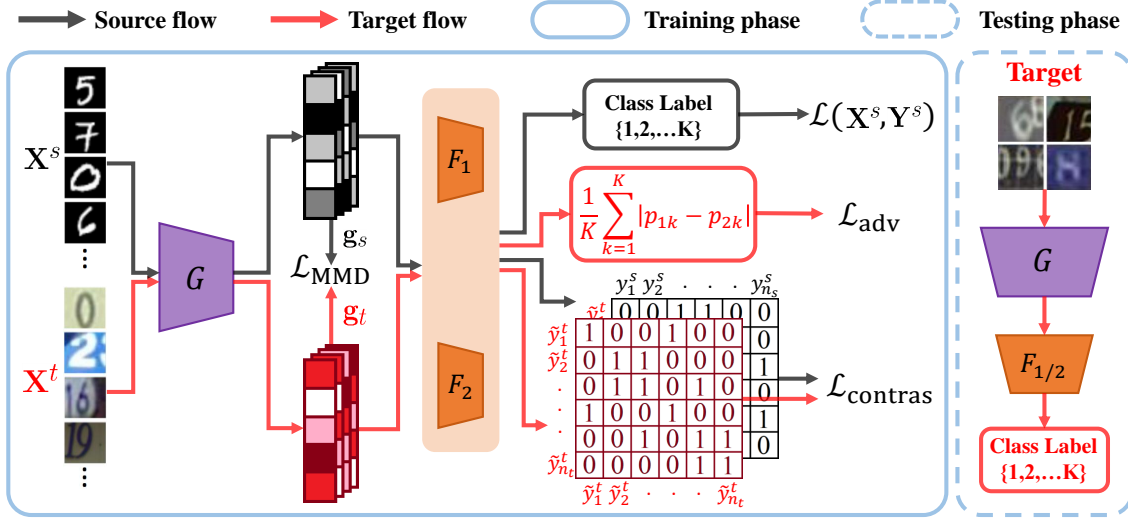


Figure 2: Framework of the proposed CoSCA. The inputs are  $\mathbf{X}^s$  with label  $\mathbf{Y}^s$  from the source domain and unlabeled  $\mathbf{X}^t$  from the target domain. The model contains a shared feature generator  $G$  and two feature classifiers  $F_1$  and  $F_2$ .  $\mathcal{L}_{\text{MMD}}$  is calculated using the generated feature mean of the source and target, *i.e.*,  $g_s$  and  $g_t$  respectively.  $\mathcal{L}_{\text{adv}}$  is the classifier discrepancy calculated based on the probability outputs  $p_1$  and  $p_2$  of  $F_1(G(\mathbf{X}^t))$  and  $F_2(G(\mathbf{X}^t))$ , respectively.  $\mathcal{L}_{\text{contras}}$  is the contrastive loss calculated for both source-and-target and target-and-target samples.

Adversarial domain adaptation approaches such as (Saito et al. 2018; Kim et al. 2019) achieve this goal via a two-step procedure: *i*) train a feature generator  $G$  and the feature classifiers  $F_1$ ,  $F_2$  with the source domain data, to ensure the generated features are class-conditional; *ii*) train  $F_1$  and  $F_2$  so that the prediction discrepancy between the two classifiers is maximized, and train  $G$  to generate features that are distinctively separated. The maximum classifier discrepancy detects the target features that are far from the support of the source domain. As the generator tries to fool the classifiers (*i.e.*, minimizing the discrepancy), these target-domain features are enforced to be categorized and aligned with the source-domain features.

However, only measuring divergence between  $F_1$  and  $F_2$  can be considered first-order moment matching, which may be insufficient for adversarial training. Previous work also observed similar issues (Arora et al. 2017; Tsai et al. 2018). We tackle this challenge by adding the Maximum Mean Discrepancy (MMD) loss, that matches the difference via higher-order moments. Also, the class alignment in existing UDA methods takes into account the intra-class domain discrepancy only, which makes it difficult to separate samples within the same class that are close to the decision boundary. Thus, in addition to the discrepancy loss, we also measure both intra- and inter-class discrepancy across domains. Specifically, we propose to minimize the distance among target-domain features that fall into the same class based on decision boundaries, and separate those features from different categories. During this process, ambiguous target features are simultaneously kept away from the decision boundaries and mapped into the high-density region, achieving better class alignment.

### Global Alignment with MMD

Following (Saito et al. 2018), we first train a feature generator  $G(\cdot)$  and two classifiers  $F_1(G(\cdot))$  and  $F_2(G(\cdot))$  to minimize the softmax cross-entropy loss using the data from the labeled source domain  $\mathcal{S}$ , defined as:

$$\mathcal{L}(\mathbf{X}^s, \mathbf{Y}^s) = -\mathbb{E}_{(\mathbf{x}^s, y^s) \sim (\mathbf{X}^s, \mathbf{Y}^s)} \left[ \sum_{k=1}^K \mathbb{1}_{[k=y^s]} \log p_1(y|\mathbf{x}^s) + \sum_{k=1}^K \mathbb{1}_{[k=y^s]} \log p_2(y|\mathbf{x}^s) \right] \quad (1)$$

where  $p_1(y|\mathbf{x})$  and  $p_2(y|\mathbf{x})$  are the probabilistic output of the two classifiers  $F_1(G(\mathbf{x}))$  and  $F_2(G(\mathbf{x}))$ , respectively.

In addition to (1), we explicitly minimize the distance between the source and target feature distributions with MMD. The main idea of MMD is to estimate the distance between two distributions as the distance between sample means of the projected embeddings in a Hilbert space. Minimizing MMD is equivalent to minimizing all orders of moments (Gretton et al. 2012). In practice, the squared value of MMD is estimated with empirical kernel mean embeddings:

$$\mathcal{L}_{\text{MMD}}(\mathbf{X}^s, \mathbf{X}^t) = \sum_{i=1}^{n_s} \sum_{j=1}^{n_t} k\left(\phi\left(\frac{\mathbf{g}_s}{\|\mathbf{g}_s\|}\right), \phi\left(\frac{\mathbf{g}_t}{\|\mathbf{g}_t\|}\right)\right) \quad (2)$$

$$\mathbf{g}_s = \frac{1}{n_s} \sum_{i=1}^{n_s} G(\mathbf{x}_i^s), \quad \mathbf{g}_t = \frac{1}{n_t} \sum_{i=1}^{n_t} G(\mathbf{x}_i^t)$$

where  $\phi(\cdot)$  is the kernel mapping,  $\mathbf{g}_s \in \mathcal{R}^n$ ,  $\mathbf{g}_t \in \mathcal{R}^n$ ,  $n_s$  and  $n_t$  denote the size of a training mini-batch of the data from the source domain  $\mathcal{S}$  and the target domain  $\mathcal{T}$ , respectively;  $\|\cdot\|$  denotes the  $\ell_2$ -norm. With the MMD loss  $\mathcal{L}_{\text{MMD}}$ , the normalized features in the two domains are encouraged to be identically distributed, leading to better global domain alignment.

## Contrastively Smoothed Class Alignment

**Discrepancy Loss.** The discrepancy loss represents the level of disagreement between the two feature classifiers in prediction for target-domain samples. Specifically, the discrepancy loss between  $F_1$  and  $F_2$  is defined as:

$$d(p_1(\mathbf{y}|\mathbf{x}), p_2(\mathbf{y}|\mathbf{x})) = \frac{1}{K} \sum_{k=1}^K |p_{1k}(\mathbf{y}|\mathbf{x}) - p_{2k}(\mathbf{y}|\mathbf{x})| \quad (3)$$

where  $|\cdot|$  denotes the  $\ell_1$ -norm, and  $p_{1k}(\cdot)$  and  $p_{2k}(\cdot)$  are the probability output of  $p_1$  and  $p_2$  for the  $k$ -th class, respectively. Accordingly, we can define the discrepancy loss over the target domain  $\mathcal{T}$ :

$$\mathcal{L}_{\text{adv}}(\mathbf{X}^t) = \mathbb{E}_{\mathbf{x}^t \sim \mathcal{T}} [d(p_1(\mathbf{y}|\mathbf{x}^t), p_2(\mathbf{y}|\mathbf{x}^t))] \quad (4)$$

Adversarial training is conducted in the Maximum Classifier Discrepancy (MCD) setup (Saito et al. 2018):

$$\begin{aligned} \min_{F_1, F_2} \mathcal{L}(\mathbf{X}^s, \mathbf{Y}^s) - \lambda \mathcal{L}_{\text{adv}}(\mathbf{X}^t) \\ \min_G \mathcal{L}_{\text{adv}}(\mathbf{X}^t) \end{aligned} \quad (5)$$

where  $\lambda$  is a hyper-parameter. Minimizing the discrepancy between the two classifiers  $F_1$  and  $F_2$  induces smoothness for the clearly classified target-domain features, while the region in the vacancy among the ambiguous ones remains non-smooth. Moreover, MCD only utilizes the unlabeled target-domain samples, while ignoring the labeled source-domain data when estimating the discrepancy.

**Contrastive Loss.** To further optimize  $G$  to estimate the underlying label hypothesis of target-domain samples, we propose to measure the intra- and inter-class discrepancy across domains, conditional on class information. By using an indicator defined as  $c(y, y') = \begin{cases} 1 & y = y' \\ 0 & y \neq y' \end{cases}$ , we define the contrastive loss between  $\mathcal{S}$  and  $\mathcal{T}$  as:

$$\mathcal{L}_{\text{contras}}^{\mathcal{S} \leftrightarrow \mathcal{T}} = \sum_{\mathbf{x}_i^s \in \mathcal{S}, \mathbf{x}_j^t \in \mathcal{T}} L_{\text{dis}}(G(\mathbf{x}_i^s), G(\mathbf{x}_j^t), c(y_i^s, \tilde{y}_j^t)) \quad (6)$$

where  $L_{\text{dis}}$  is a distance measure (defined below), and  $\tilde{y}_j^t$  is the predicted target label for  $\mathbf{x}_j^t$ . Specifically, (6) covers two types of class-aware domain discrepancies: *i*) intra-class domain discrepancy ( $y_i^s = \tilde{y}_j^t$ ); and *ii*) inter-class domain discrepancy ( $y_i^s \neq \tilde{y}_j^t$ ). Note that  $y_i^s$  is known, providing some supervision for parameter learning. Similarly, we can define the constrastive loss between  $\mathcal{T}$  and  $\mathcal{S}$  as:

$$\mathcal{L}_{\text{contras}}^{\mathcal{T} \leftrightarrow \mathcal{S}} = \sum_{\mathbf{x}_i^t, \mathbf{x}_j^s \in \mathcal{S}} L_{\text{dis}}(G(\mathbf{x}_i^t), G(\mathbf{x}_j^s), c(\tilde{y}_i^t, y_j^s)) \quad (7)$$

To obtain the indicator  $c(y, y')$ , estimated target label  $\tilde{y}_i^t$  is required. Specifically, for each data sample  $\mathbf{x}_j^t$ , a pseudo label is predicted based on the maximum posterior probability of the two classifiers:

$$\begin{aligned} \tilde{y}_j^t = \arg \max_{k \in \{1, 2, \dots, K\}} \left\{ p(F_1(G(\mathbf{x}_j^t)) = k | \mathbf{x}) \right. \\ \left. + p(F_2(G(\mathbf{x}_j^t)) = k | \mathbf{x}) \right\} \end{aligned} \quad (8)$$

---

## Algorithm 1 Training procedure of CoSCA.

---

- 1: **Input:** Source domain samples  $\{\mathbf{x}_i^s, y_i^s\}$ , and target domain samples  $\{\mathbf{x}_j^t\}$ . Inner-loop iteration  $\tau$  and  $\delta$ .
  - 2: **Output:** Classifiers  $F_1$  and  $F_2$ , and generator  $G$ .
- 
- 3: **for**  $iter$  from 1 to  $max\_iter$  **do**
  - 4:   Sample a mini-batch of source samples  $[\mathbf{x}_i^s, y_i^s]$  and target samples  $[\mathbf{x}_j^t]$ .
  - 5:   Compute  $\mathcal{L}(\mathbf{X}^s, \mathbf{Y}^s)$  on  $[\mathbf{x}_i^s, y_i^s]$ .
  - 6:   Compute  $\mathcal{L}_{\text{MMD}}(\mathbf{X}^s, \mathbf{X}^t)$  on  $[\mathbf{x}_i^s, \mathbf{x}_j^t]$ .
  - 7:   Update  $G$ ,  $F_1$  and  $F_2$  using (11).
  - 8:   **for**  $inner\_loop\_iter_1$  from 1 to  $\tau$  **do**
  - 9:     Compute  $\mathcal{L}(\mathbf{X}^s, \mathbf{Y}^s)$  on  $[\mathbf{x}_i^s, y_i^s]$ .
  - 10:    Compute  $\mathcal{L}_{\text{adv}}(\mathbf{X}^t)$  on  $\mathbf{x}_j^t$ .
  - 11:    Fix  $G$ , update  $F_1$  and  $F_2$  using (12).
  - 12:   **end for**
  - 13:   **for**  $inner\_loop\_iter_2$  from 1 to  $\delta$  **do**
  - 14:     Compute  $\mathcal{L}_{\text{adv}}(\mathbf{X}^t)$  on  $\mathbf{x}_j^t$ .
  - 15:     Compute  $\mathcal{L}_{\text{contras}}(\mathbf{X}^s, \mathbf{Y}^s, \mathbf{X}^t)$  on  $[\mathbf{x}_i^s, y_i^s, \mathbf{x}_j^t]$ .
  - 16:     Fix  $F_1$  and  $F_2$ , update  $G$  using (13).
  - 17:   **end for**
  - 18: **end for**
- 

Ideally, based on the indicator,  $L_{\text{dis}}$  should ensure the gathering of features that fall in the same class, while separating those in different categories. Following (Luo et al. 2017), we utilize contrastive Siamese networks (Bromley et al. 1994), which can learn an invariant mapping to a smooth and coherent feature space and perform well in practice:

$$L_{\text{dis}} = \begin{cases} \|G(\mathbf{x}_i) - G(\mathbf{x}_j)\|^2 & c_{ij} = 1 \\ \max(0, m - \|G(\mathbf{x}_i) - G(\mathbf{x}_j)\|)^2 & c_{ij} = 0 \end{cases} \quad (9)$$

where  $c_{ij} = c(y_i, y_j)$  and  $m$  is a pre-defined margin. The margin loss constrains the neighboring features to be consistent. Based on the above definitions of source-and-target and target-and-target contrastive losses, the overall objective is obtained:

$$\mathcal{L}_{\text{contras}}(\mathbf{X}^s, \mathbf{Y}^s, \mathbf{X}^t) = \mathcal{L}_{\text{contras}}^{\mathcal{S} \leftrightarrow \mathcal{T}} + \mathcal{L}_{\text{contras}}^{\mathcal{T} \leftrightarrow \mathcal{S}} \quad (10)$$

Minimizing the contrastive loss  $\mathcal{L}_{\text{contras}}$  encourages features in the same class to aggregate together while pushing unrelated pairs away from each other. In other words, the semantic feature approximation is enhanced to induce smoothness between data in the feature space.

## Training Procedure

We need to optimize  $G$ ,  $F_1$  and  $F_2$  by combining all the aforementioned losses, performed in an adversarial training manner. Specifically, we first train the classifiers  $F_1$  and  $F_2$  and the generator  $G$  to minimize the objective:

$$\min_{F_1, F_2, G} \mathcal{L}(\mathbf{X}^s, \mathbf{Y}^s) + \lambda_1 \mathcal{L}_{\text{MMD}}(\mathbf{X}^s, \mathbf{X}^t) \quad (11)$$

We then train the classifiers  $F_1$  and  $F_2$  while keeping the generator  $G$  fixed. The objective is:

$$\min_{F_1, F_2} \mathcal{L}(\mathbf{X}^s, \mathbf{Y}^s) - \lambda_2 \mathcal{L}_{\text{adv}}(\mathbf{X}^t) \quad (12)$$

Lastly, we train the generator  $G$  with the following objective, while keeping both  $F_1$  and  $F_2$  fixed:

$$\min_G \lambda_2 \mathcal{L}_{\text{adv}}(\mathbf{X}^t) + \lambda_3 \mathcal{L}_{\text{contras}}(\mathbf{X}^s, \mathbf{Y}^s, \mathbf{X}^t) \quad (13)$$

where  $\lambda_1$ ,  $\lambda_2$  and  $\lambda_3$  are hyper-parameters that balance the different objectives. These steps are repeated, with the full algorithm summarized in Algorithm 1. In our experiments, the inner-loop iteration numbers  $\tau$  and  $\delta$  are both set to 2.

**Class-aware sampling.** When training with the contrastive loss, it is important to sample a mini-batch of data with all the classes, to allow (10) to be fully trained. We propose to use a class-aware sampling strategy to enable efficient update of the network. Specifically, we randomly select a subset of classes and then sample data from each class. Consequently, in each mini-batch of the data, we are able to estimate the intra/inter-class discrepancy for each selected class.

**Dynamic parameterization of  $\lambda_3$ .** In our implementation, we adapt a dynamic  $\omega(t)$  to parameterize  $\lambda_3$ . We set  $\omega(t) = \exp[-\theta(1 - \frac{t}{\text{max-epochs}})]\lambda_3$ , which is a Gaussian curve ranging from 0 to  $\lambda_3$ . This is to prevent unlabeled target features gathering in the early stage of training, as the pseudo labels might not be reliable.

## Experiments

We evaluate the proposed model mainly on image datasets. To compare with MCD (Saito et al. 2018) as well as the state-of-the-art results in (Shu et al. 2018; Kumar et al. 2018), we evaluate on the same datasets used in those studies: the digit datasets (*i.e.*, MNIST, MNISTM, Street View House Numbers (SVHN), and USPS), CIFAR-10, and STL-10. We also conduct experiments on the VisDA dataset, *i.e.*, large-scale images. Our model can also be applied to non-visual domain adaptation tasks. Specifically, to show the flexibility of our model, we also evaluate it on the Amazon Reviews dataset.

For visual domain adaptation tasks, the proposed model is implemented based on VADA (Shu et al. 2018) and Co-DA (Kumar et al. 2018) to avoid any incidental difference caused by network architecture. However, different from these models, our model does not require a discriminator, and only adopts the architecture for the feature generator  $G$  and the classifier  $F$ . We also include instance normalization (Shu et al. 2018; Ulyanov et al. 2016), achieving superior results on several benchmarks. For the VisDA dataset, we implemented our model based on the codebase of self-ensembling domain adaptation (SEDA) (French et al. 2018). To compare with MCD (Saito et al. 2018), we re-implemented it using the exact architecture as our model.

In addition to the aforementioned baseline models, we also include the results from recently proposed unsupervised domain adaptation models. Note that standard domain adaptation methods (such as Transfer Component Analysis (TCA) (Pan et al. 2011) and Subspace Alignment (SA) (Fernando et al. 2013)) are not included; these models only work on pre-extracted features, and are often not scalable to large datasets. Instead, we mainly compare our model with methods based on adversarial neural networks.

For the non-visual task, we adopt a one-layer CNN structure from previous work (Kim 2014). The feature generator  $G$  consists of three components, including a 300-dimensional word embedding layer using GloVe (Pennington et al. 2014), a one-layer CNN with ReLU, and a max-over-time pooling through which the final sentence representation is obtained. The classifiers  $F_1$  and  $F_2$  can be decomposed into one dropout layer and one fully connected output layer.

## Digit Datasets

There are four types of digit images (*i.e.*, four domains). MNIST and USPS are both hand-written gray-scale images, the domain difference between which is relatively small. MNISTM (Ganin et al. 2016) is a dataset built upon MNIST by adding randomly colored image patches from BSD500 dataset (Arbelaez et al. 2011). SVHN includes colored images of street numbers. All images are rescaled to  $32 \times 32 \times 3$ .

**MNIST→SVHN.** As gray-scale handwritten digits, images from MNIST has much lower dimensionality than those colored house numbers from SVHN. With such large domain gap, MCD fails to align the features of the two. Figure 3(a) plots the t-SNE embedding of the features learned by MCD. Domains are indicated by different colors, and classes are indicated by different digit numbers. The maximized discrepancy provides too many ambiguous target-domain samples. As a result, the feature generator may not properly align them with the source-domain samples. In comparison, as shown in Figure 3(b), CoSCA utilizes the MMD between the source and the target domain features, thus maintaining a better global domain alignment. With further smoothed class-conditional adaptation, it achieves test accuracy of 80.7%, as shown in Table 1, competitive with state-of-the-art results from (Kumar et al. 2018).

**SVHN→MNIST.** Classification with the MNIST dataset is easier than others. As shown in the table, source-only achieves 82.4% on SVHN→MNIST with instance normalization. Therefore, even with the same amount of domain difference, performance on SVHN→MNIST is much better than MNIST→SVHN across all compared models. The test accuracy of our model achieves 98.7%.

**MNIST→MNISTM.** Since MNISTM is a colored version of MNIST, there exists a one-to-one matching between the two datasets, *i.e.*, a domain adaptation model would perform well as long as domain-invariant features are properly extracted. CoSCA provides better results than Co-DA, yielding a test accuracy of 98.9%.

**MNIST→USPS.** Evaluation on MNIST and USPS datasets is also conducted to compare our model with other baselines. Ours achieves a superb result of 99.3%.

## CIFAR-10 and STL-10 Datasets

CIFAR-10 and STL-10 are both 10-class datasets, with each image containing an animal or a type of transportation. Images from each class are much more diverse than the digit datasets, with higher intrinsic dimensionality, which makes it a harder domain adaptation task. There are 9 overlapping classes between these two datasets. CIFAR provides

Source Domain Target Domain	MNIST SVHN	SVHN MNIST	MNIST MNISTM	MNIST USPS	CIFAR STL	STL CIFAR
MMD (Long et al. 2015)	-	71.1	76.9	81.1	-	-
DANN (Ganin et al. 2016)	35.7	71.1	81.5	77.1	-	-
DSN (Bousmalis et al. 2016)	40.1	82.7	83.2	91.3	-	-
ATT (Saito et al. 2017b)	52.8	86.2	94.2	-	-	-
With Instance-Normalized Input:						
Source-Only	40.9	82.4	59.9	76.7	77.0	62.6
VADA (Shu et al. 2018)	73.3	94.5	95.7	-	78.3	71.4
Co-DA (Kumar et al. 2018)	<b>81.3</b>	98.6	97.3	-	80.3	74.5
MCD (Saito et al. 2018)	68.7	96.2 <sup>†</sup>	96.7	94.2 <sup>†</sup>	78.1	69.2
CoSCA	80.7	<b>98.7</b>	<b>98.9</b>	<b>99.3</b>	<b>81.7</b>	<b>75.2</b>

Table 1: Results on visual domain adaptation tasks. Source-Only means to train a classifier in the source domain and apply it directly to the target domain without any adaptation. Results with <sup>†</sup> are reported in (Saito et al. 2018).

Model	plane	bcycl	bus	car	horse	knife	mcycl	person	plant	sktbrd	train	truck	mean
Source Only	55.1	53.3	61.9	59.1	80.6	17.9	79.7	31.2	81.0	26.5	73.5	8.5	52.4 <sup>†</sup>
MMD (Long et al. 2015)	87.1	63.0	76.5	42.0	90.3	42.9	85.9	53.1	49.7	36.3	85.8	20.7	61.1 <sup>†</sup>
DANN (Ganin et al. 2016)	81.9	77.7	82.8	44.3	81.2	29.5	65.1	28.6	51.9	54.6	82.8	7.8	57.4 <sup>†</sup>
MCD (Saito et al. 2018)	89.1	80.8	82.9	70.9	91.6	56.5	89.5	79.3	90.9	76.1	88.3	29.3	77.1
SEDA (French et al. 2018)	95.3	87.1	84.2	58.3	94.4	<b>89.6</b>	87.9	79.1	92.8	<b>91.3</b>	<b>89.6</b>	<b>37.4</b>	82.2
CoSCA	<b>95.7</b>	<b>87.4</b>	<b>85.7</b>	<b>73.5</b>	<b>95.3</b>	72.8	<b>91.5</b>	<b>84.8</b>	<b>94.6</b>	87.9	87.9	36.8	<b>82.9</b>

Table 2: Test accuracy of ResNet101 model fine-tuned on the VisDA dataset. Results with <sup>†</sup> are reported in (Saito et al. 2018).

images of size  $32 \times 32$  and a large training set of 50,000 image samples, while STL contains higher quality images of size  $96 \times 96$ , but with a much smaller training set of 5,000 samples. Following (French et al. 2018; Shu et al. 2018; Kumar et al. 2018), we remove non-overlapping classes from these two datasets and resize the images from STL to  $32 \times 32$ .

Due to the small training set in STL, STL→CIFAR is more difficult than CIFAR→STL. For the latter, the source-only model with no adaptation involved achieves an accuracy of 77.0%. With adaptation, the margin-of-improvement is relatively small, while CoSCA provides the best improvement of 4.7% among all the models (Table 1). For STL→CIFAR, our model yields a 12.6% margin-of-improvement and an accuracy of 75.2%. Figures 3(c) and 3(d) provide t-SNE plots for MCD and our model, respectively, which shows our model achieves much better alignment for each class.

### VisDA Dataset

The VisDA dataset is a large-scale image dataset that evaluates the adaptation from synthetic-object to real-object images. Images from the source domain are synthetic renderings of 3D models from different angles and lighting conditions. There are 152,397 image samples in the source domain, and 55,388 image samples in the target domain. The image size, after rescaling as in (Saito et al. 2018), is  $224 \times 224 \times 3$ . A model architecture with ResNet101 (He et al. 2016) pre-trained on Imagenet is required. There are 12 different object categories in VisDA, shared by the source and the target domains.

Table 2 shows the test accuracy of different models in all object classes. The class-aware methods, namely MCD (Saito et al. 2018), SEDA (French et al. 2018), and our proposed CoSCA, outperforms the source only model in all categories. In comparison, the methods that are mainly based on distribution matching do not perform well in some of the categories. CoSCA outperforms MCD, showing the effectiveness of contrastive loss and MMD global alignment. In addition, it performs better than SEDA in most categories, demonstrating its robustness in handling large scale images.

### Text Dataset

We also evaluate CoSCA on the Amazon Reviews dataset collected by (Blitzer et al. 2007). It contains reviews from several different domains, with 1000 positive and 1000 negative reviews in each domain.

Model	Accuracy
Source-Only	79.13
DANN (Ganin et al. 2016)	80.29
PBLM (Ziser and Reichart 2018)	80.40 <sup>†</sup>
MCD (Saito et al. 2018)	81.35
DAS (He et al. 2018)	81.96 <sup>†</sup>
CoSCA	<b>83.17</b>

Table 3: Results on the text classification task. Results with <sup>†</sup> are reported by (He et al. 2018; Ziser and Reichart 2018).

Table 3 shows the average classification accuracy of different methods. We use the same model architecture and parameter setting for MCD and the source-only model. Results



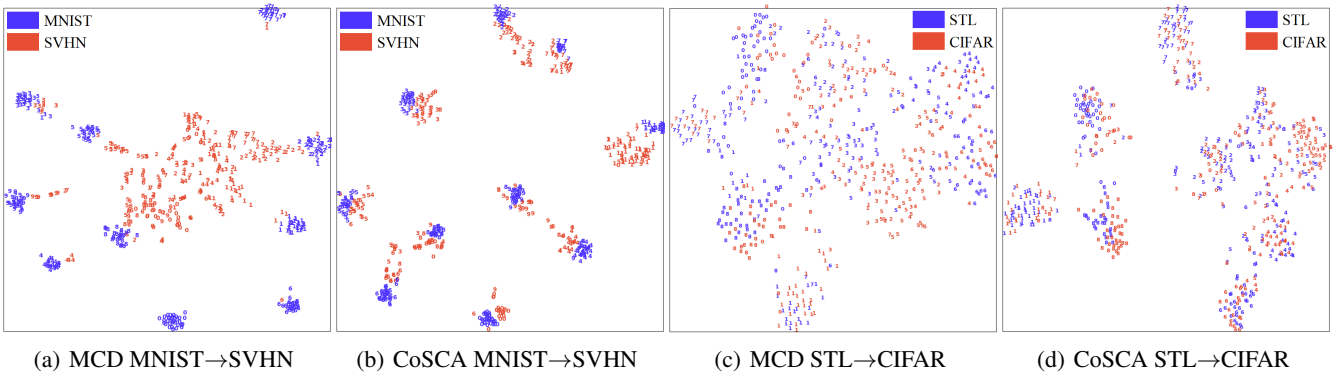


Figure 3: t-SNE embedding of the features  $G(x)$  for MNIST→SVHN and STL→CIFAR. Color indicates domain, and the digit number is the label. The ideal situation is to mix the two colors with the same label, representing domain-invariant features. The t-SNE plots for the other datasets are provided in Supplementary Material.

Model	MNIST SVHN	STL CIFAR	Amazon Reviews
MCD (Saito et al. 2018)	68.7	69.2	81.35
MCD+MMD	72.1	70.2	81.73
MCD+Contras	75.9	73.4	82.56
CoSCA	<b>80.7</b>	<b>75.2</b>	<b>83.17</b>

Table 4: Ablation study on CoSCA with different variations of MCD on MNIST→SVHN, STL→CIFAR, and Amazon Reviews.

show that the proposed CoSCA outperforms all other methods. Specifically, it improves the performance from test accuracy of 81.96% to 83.17%, when comparing to the state-of-the-art method DAS. MCD achieves 81.35%, also outperformed by CoSCA.

### Ablation Study

To further demonstrate the improvement of CoSCA over MCD (Saito et al. 2018), we conduct ablation studies. Specifically, with the same network architecture and setup, we compare model performance among 1) MCD, 2) MCD with only smooth alignment (MCD+Contras), 3) MCD with only global alignment (MCD+MMD), and 4) CoSCA, to validate the effectiveness of adding contrastive loss  $\mathcal{L}_{\text{contras}}$  and MMD loss  $\mathcal{L}_{\text{MMD}}$  to MCD. As MCD has already achieved great performance on some of the benchmark datasets, we mainly choose those tasks on which MCD does not perform very well, in order to better analyze the margin-of-improvement. Therefore, MNIST→SVHN, STL→CIFAR, and Amazon Reviews are selected for this experiment, and the results are provided in Table 4.

**Effect of Contrastive Alignment.** We compare CoSCA with MCD as well as its few variations, to validate the effectiveness of the proposed contrastive alignment. Table 4 provides the test accuracy for every model across the selected benchmark datasets. For MNIST→SVHN, MCD+Contrastive outperforms MCD by 7.2%. For STL→CIFAR and Amazon Reviews, the margin-of-improvement is 4.2% and 1.21%, respectively (less significant than MNIST→SVHN, possibly due to the smaller domain difference). Note that the results of MCD+Contras are still worse than CoSCA, demonstrating

the effectiveness of the global domain alignment and the framework design of our model.

**Effect of MMD.** We further investigate how the MMD loss can impact the performance of our proposed CoSCA. Specifically, MCD+MMD achieves a test accuracy of 72.1% for MNIST→SVHN, only lifting the original result of MCD by 3.4%. For STL→CIFAR and Amazon Reviews, the margin-of-improvement is 1.0% and 0.38%, respectively. While this validates the effectiveness of having global alignment in the MCD framework, the improvement is small. Without a smoothed class-conditional alignment, MCD still encounters misclassified target features during training, leading to a sub-optimal solution. Notice that when comparing CoSCA with MCD+Contras, the improvement is significant for MNIST→SVHN, with validation accuracy and training stability enhanced. This demonstrates the importance of global alignment when there exists a large domain difference.

### Conclusions

We have proposed Contrastively Smoothed Class Alignment (CoSCA) for the UDA problem, by explicitly combining intra-class and inter-class domain discrepancy and optimizing class alignment through end-to-end training. Experiments on several benchmarks demonstrate that our model can outperform state-of-the-art baselines. Our experimental analysis shows that CoSCA learns more discriminative target-domain features, and the introduced MMD feature matching improves the global domain alignment. For future work, we want to develop a theoretical interpretation of contrastive learning for domain adaptation, particularly characterizing its effects on the alignment of source and target domain feature distributions.

### References

- Arbelaez, P.; Maire, M.; Fowlkes, C.; and Malik, J. 2011. Contour detection and hierarchical image segmentation. *PAMI*.
- Arora, S.; Ge, R.; Liang, Y.; Ma, T.; and Zhang, Y. 2017. Generalization and equilibrium in generative adversarial nets (GANs). In *ICML*.

- Blitzer, J.; Dredze, M.; and Pereira, F. 2007. Domain adaptation for sentiment classification. In *ACL*.
- Bousmalis, K.; Trigeorgis, G.; Silberman, N.; Krishnan, D.; and Erhan, D. 2016. Domain separation networks. In *NeurIPS*.
- Bromley, J.; Guyon, I.; LeCun, Y.; Säckinger, E.; and Shah, R. 1994. Signature verification using a "siamese" time delay neural network. In *NeurIPS*.
- Chapelle, O.; Scholkopf, B.; and Zien, A. 2009. Semi-supervised learning. *IEEE Transactions on Neural Networks*.
- Dai, B., and Lin, D. 2017. Contrastive learning for image captioning. In *NeurIPS*.
- Donahue, J.; Jia, Y.; Vinyals, O.; Hoffman, J.; Zhang, N.; Tzeng, E.; and Darrell, T. 2014. Decaf: A deep convolutional activation feature for generic visual recognition. In *ICML*.
- Fernando, B.; Habrard, A.; Sebban, M.; and Tuytelaars, T. 2013. Unsupervised visual domain adaptation using subspace alignment. In *ICCV*.
- French, G.; Mackiewicz, M.; and Fisher, M. 2018. Self-ensembling for domain adaptation. In *ICLR*.
- Ganin, Y., and Lempitsky, V. 2014. Unsupervised domain adaptation by backpropagation. *arXiv preprint arXiv:1409.7495*.
- Ganin, Y.; Ustinova, E.; Ajakan, H.; Germain, P.; Larochelle, H.; Laviolette, F.; Marchand, M.; and Lempitsky, V. 2016. Domain-adversarial training of neural networks. *JMLR*.
- Goodfellow, I.; Pouget-Abadie, J.; Mirza, M.; Xu, B.; Warde-Farley, D.; Ozair, S.; Courville, A.; and Bengio, Y. 2014. Generative adversarial nets. In *NeurIPS*.
- Gretton, A.; Smola, A. J.; Huang, J.; Schmittfull, M.; Borgwardt, K. M.; and Schölkopf, B. 2009. Covariate shift by kernel mean matching. In *MIT press*.
- Gretton, A.; Borgwardt, K. M.; Rasch, M. J.; Schölkopf, B.; and Smola, A. 2012. A kernel two-sample test. *JMLR*.
- Hadsell, R.; Chopra, S.; and LeCun, Y. 2006. Dimensionality reduction by learning an invariant mapping. In *CVPR*.
- Haeusser, P.; Frerix, T.; Mordvintsev, A.; and Cremers, D. 2017. Associative domain adaptation. In *ICCV*.
- He, K.; Zhang, X.; Ren, S.; and Sun, J. 2016. Deep residual learning for image recognition. In *CVPR*.
- He, R.; Lee, W. S.; Ng, H. T.; and Dahlmeier, D. 2018. Adaptive semi-supervised learning for cross-domain sentiment classification. In *ACL*.
- Kang, G.; Jiang, L.; Yang, Y.; and Hauptmann, A. G. 2019. Contrastive adaptation network for unsupervised domain adaptation. In *CVPR*.
- Kim, M.; Sahu, P.; Gholami, B.; and Pavlovic, V. 2019. Unsupervised visual domain adaptation: A deep max-margin gaussian process approach. *arXiv preprint arXiv:1902.08727*.
- Kim, Y. 2014. Convolutional neural networks for sentence classification. In *EMNLP*.
- Kumar, A.; Sattigeri, P.; Wadhawan, K.; Karlinsky, L.; Feris, R.; Freeman, B.; and Wornell, G. 2018. Co-regularized alignment for unsupervised domain adaptation. In *NeurIPS*.
- Li, C.; Xu, K.; Zhu, J.; and Zhang, B. 2017. Triple generative adversarial nets. In *NeurIPS*.
- Long, M.; Cao, Y.; Wang, J.; and Jordan, M. 2015. Learning transferable features with deep adaptation networks. In *ICML*.
- Long, M.; Zhu, H.; Wang, J.; and Jordan, M. I. 2016. Unsupervised domain adaptation with residual transfer networks. In *NeurIPS*.
- Long, M.; CAO, Z.; Wang, J.; and Jordan, M. I. 2018. Conditional adversarial domain adaptation. In *NeurIPS*.
- Luo, Y.; Zhu, J.; Li, M.; Ren, Y.; and Zhang, B. 2017. Smooth neighbors on teacher graphs for semi-supervised learning. In *CVPR*.
- Pan, S. J.; Yang, Q.; et al. 2010. A survey on transfer learning. *IEEE Transactions on knowledge and data engineering*.
- Pan, S. J.; Tsang, I. W.; Kwok, J. T.; and Yang, Q. 2011. Domain adaptation via transfer component analysis. *IEEE Transactions on Neural Networks*.
- Pei, Z.; Cao, Z.; Long, M.; and Wang, J. 2018. Multi-adversarial domain adaptation. In *AAAI*.
- Pennington, J.; Socher, R.; and Manning, C. 2014. Glove: Global vectors for word representation. In *EMNLP*.
- Rifai, S.; Dauphin, Y. N.; Vincent, P.; Bengio, Y.; and Muller, X. 2011. The manifold tangent classifier. In *NeurIPS*.
- Saito, K.; Ushiku, Y.; Harada, T.; and Saenko, K. 2017a. Adversarial dropout regularization. *arXiv preprint arXiv:1711.01575*.
- Saito, K.; Ushiku, Y.; and Harada, T. 2017b. Asymmetric tri-training for unsupervised domain adaptation. In *ICML*.
- Saito, K.; Watanabe, K.; Ushiku, Y.; and Harada, T. 2018. Maximum classifier discrepancy for unsupervised domain adaptation. In *CVPR*.
- Sener, O.; Song, H. O.; Saxena, A.; and Savarese, S. 2016. Learning transferrable representations for unsupervised domain adaptation. In *NeurIPS*.
- Shu, R.; Bui, H. H.; Narui, H.; and Ermon, S. 2018. A dirt-t approach to unsupervised domain adaptation. In *ICLR*.
- Simonyan, K., and Zisserman, A. 2015. Very deep convolutional networks for large-scale image recognition. In *ICLR*.
- Torralba, A., and Efros, A. A. 2011. Unbiased look at dataset bias. In *CVPR*.
- Tsai, Y.-H.; Hung, W.-C.; Schulter, S.; Sohn, K.; Yang, M.-H.; and Chandraker, M. 2018. Learning to adapt structured output space for semantic segmentation. In *CVPR*.
- Tzeng, E.; Hoffman, J.; Darrell, T.; and Saenko, K. 2015. Simultaneous deep transfer across domains and tasks. In *ICCV*.
- Tzeng, E.; Hoffman, J.; Saenko, K.; and Darrell, T. 2017. Adversarial discriminative domain adaptation. In *CVPR*.
- Ulyanov, D.; Vedaldi, A.; and Lempitsky, V. 2016. Instance normalization: The missing ingredient for fast stylization. *arXiv preprint arXiv:1607.08022*.
- Wang, J.; Song, Y.; Leung, T.; Rosenberg, C.; Wang, J.; Philbin, J.; Chen, B.; and Wu, Y. 2014. Learning fine-grained image similarity with deep ranking. In *CVPR*.
- Yosinski, J.; Clune, J.; Bengio, Y.; and Lipson, H. 2014. How transferable are features in deep neural networks? In *NeurIPS*.
- Ziser, Y., and Reichart, R. 2018. Pivot based language modeling for improved neural domain adaptation. In *ACL*.
- Zou, J. Y.; Hsu, D. J.; Parkes, D. C.; and Adams, R. P. 2013. Contrastive learning using spectral methods. In *NeurIPS*.